Surface & Coatings Technology 364 (2019) 231–238

Contents lists available at ScienceDirect

Surface & Coatings Technology

journal homepage: www.elsevier.com/locate/surfcoat

Nickel fluoride as a surface activation agent for electroless nickel coating of anodized AA1050 aluminum alloy

M. Kocabaş[a,b,c,*], C. Örnek[d], M. Curioni[e], N. Cansever[c]

[a] Konya Technical University, Faculty of Engineering and Natural Sciences, Department of Metallurgical and Materials Engineering, 42075 Konya, Turkey
[b] Selçuk University, Faculty of Engineering, Department of Metallurgical and Materials Engineering, 42075 Konya, Turkey
[c] Yildiz Technical University, Faculty of Chemistry-Metallurgy, Metallurgical and Materials Engineering Department, 34210 Istanbul, Turkey
[d] KTH Royal Institute of Technology, School of Engineering Sciences in Chemistry, Biotechnology and Health, Division of Surface and Corrosion Science, Drottning Kristinas Väg 51, 10044 Stockholm, Sweden
[e] University of Manchester, School of Materials, Corrosion and Protection Centre, M139PL Manchester, United Kingdom

ARTICLE INFO

Keywords:
Nickel fluoride tetrahydrate ($NiF_2{\cdot}4H_2O$)
Aluminum alloy
Anodizing
Electroless nickel-phosphorus coating (Ni-P)
Surface activation
Scratch test

ABSTRACT

In this study, the use of nickel fluoride tetrahydrate ($NiF_2{\cdot}4H_2O$) as a surface activator and sealant at the same time for the coating of electroless nickel-phosphorus (Ni-P) on anodized aluminum alloy AA1050 is proposed. The usage of the activator resulted in more efficient deposition of Ni-P, improved adhesion properties, and increased wear and friction behavior as opposed to non-activated conditions. Scanning electron microscopy (SEM) and confocal laser microscopy (CLM) analyses of ultramicrotome-cut cross sections of Ni-P coated specimens, surface-activated by $NiF_2{\cdot}4H_2O$, revealed a more well-structured metal-coating interface as opposed to non-activated conditions.

1. Introduction

Anodic oxidation and electroless Ni-P coatings are widely used to improve the surface properties of aluminum and its alloys for a wide range of applications, including automotive, aviation, and aerospace industries. Ni-P coatings are selected due to their cost-effective magnetic and lubrication properties, which are required, for example, in plastic molding and electronic applications, with its quality being determined by the adhesion behavior with the substrate [1–3]. These coatings do not require the use of an electrical current to deposit nickel-based films, since the reducing agents in the bath provide the electrons required to reduce nickel ions [4–6].

Electroless Ni-P is either coated directly or after pre-treatments using surface activators [3,4]. However, coatings without pre-treatments do often not give satisfactory results [7] due to rapid oxidation of the alloy surface, leading to the formation of a thin surface-oxide film, which reduces adhesive forces between the metal and the coating [7,8]. Therefore, electroless Ni-P coating of aluminum alloys, generally, requires pre-treatments using activators prior to the coating process [1–3,7–20].

Pre-treatments are classified into two categories: (i) single and (ii) double pre-treatments. Zincating is the most common single pre-treatment, involving the formation of a zinc film on the aluminum substrate by a displacement reaction between aluminum and zinc ions, providing a good base for subsequent electroless Ni-P coating [2,7,12,15,18]. However, zincated Ni-P coatings can easily produce flaky structures and degrade over time due to zinc corrosion occurring upon contact with water (both in wet or atmospheric conditions) [2,7,8,11], or already during the coating process by the excessive dissolution of aluminum in the aqueous zinc bath [2,13,16]. Anodizing can also be considered as a single pre-treatment, which is often used as a precursor step for the deposition of electroless Ni-P [1,2,19,21,22], or performed with the aim as the first step in double pre-treatments [3,20].

Double pre-treatments usually consist of anodic oxidation of the aluminum substrate, followed by immersion in a solution containing either zinc, cadmium, or palladium. The purpose of the latter is to activate the surface for depositing nickel and to produce coatings with improved mechanical properties, this is because anodic oxidation is not enough to achieve good adhesion properties and high deposition rates [3]. Hence, double pre-treatment using cadmium or palladium solutions after anodic oxidation is less efficient and is also an expensive step [3,20]. Zincating, for example, has been shown to improve the adhesion of electroless coated nickel to the substrate as contrasted to anodically

* Corresponding author at: Selçuk University, Faculty of Engineering, Department of Metallurgical and Materials Engineering, 42075 Konya, Turkey.
E-mail addresses: mustafakocabas@selcuk.edu.tr (M. Kocabaş), ornek@kth.se (C. Örnek), michele.curioini@manchester.ac.uk (M. Curioni), cansev@yildiz.edu.tr (N. Cansever).

https://doi.org/10.1016/j.surfcoat.2019.03.003
Received 2 October 2018; Received in revised form 25 January 2019; Accepted 2 March 2019
Available online 04 March 2019
0257-8972/

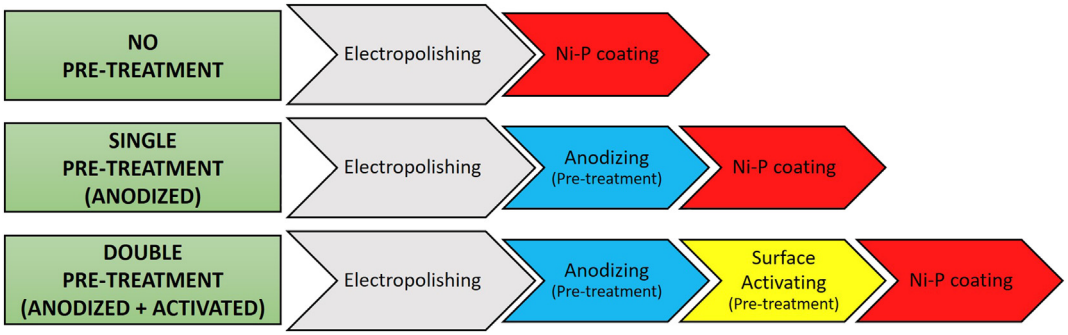

Fig. 1. Pre-treatment procedure for the coating of electroless Ni-P performed in this work.

Table 1
Constituents of the bath for coating of electroless Ni-P (pH 4.4–4.8).

Chemical	Formula	Concentration
Nickel sulfate	$NiSO_4 \cdot 6H_2O$	27 g/l
Sodium hypophosphite	$Na_2H_2PO_2 \cdot H_2O$	22 g/l
Lactic acid	$C_3H_6O_3$	27 g/l
Propionic acid	$C_3H_6O_2$	2.2 g/l
Thiourea	CH_4N_2S	1 mg/l

oxidized aluminum but is a more time-consuming step showing also less controllable structural properties [19]. Palladizing, on the other hand, has been shown to provide good morphological and structural results regarding to nickel deposition with adhesion properties, however, showing weaker performance [20]. This demonstrated the importance of a procedure to coat electroless nickel in a more efficient way, that is to achieve good mechanical properties and being still economic and sustainable at the same time. In this work, we demonstrate the advantages of using aqueous nickel fluoride as both a surface activator and a sealing agent for the deposition of electroless nickel in a rapid, efficient, and sustainable way. Nickel fluoride has been used as a sealing agent as the final step of anodizing to close pores in the aluminum oxide structure [22–26] but has never been employed with the purpose as an activator.

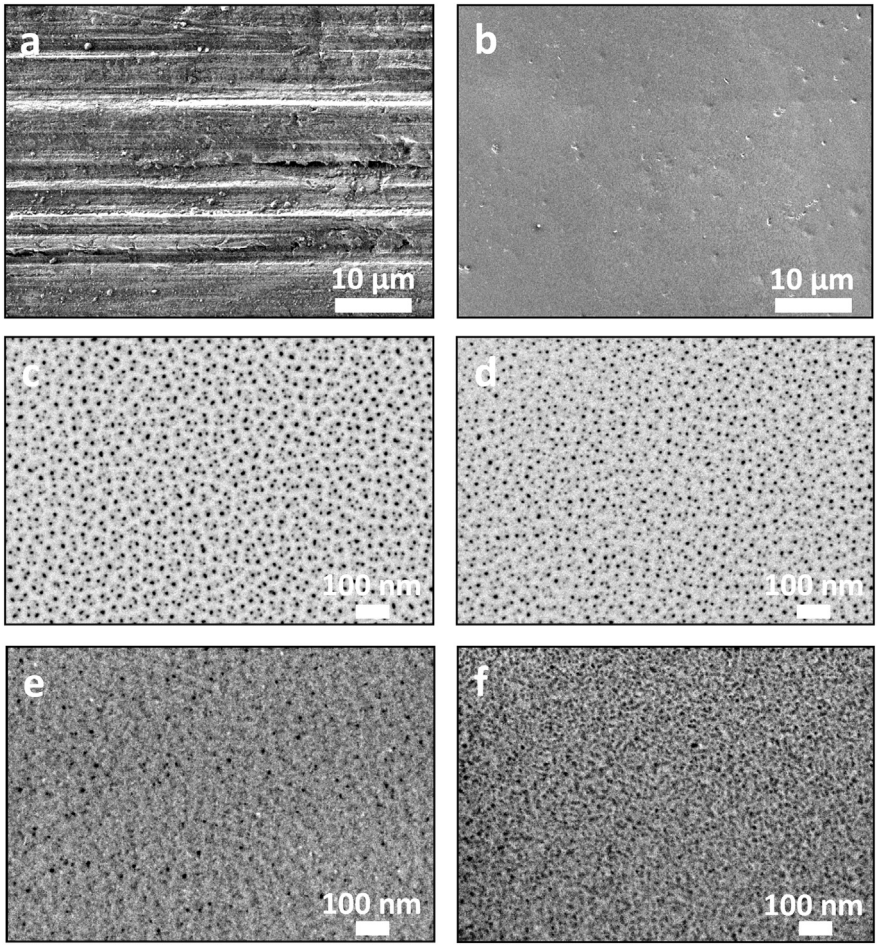

Fig. 2. SEM images showing the surface (a) before and (b) after electropolishing, (c) after anodizing, (d) after anodizing followed by immersion in nickel fluoride (sealing) for 60 s, (e) for 120 s, and (f) for 240 s.

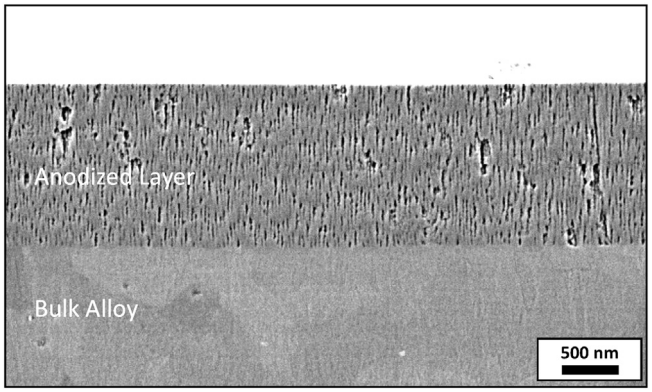

Fig. 3. Cross-sectional view (SEM image) showing the microstructure of the bulk alloy and anodized layer after surface activation for 120 s.

2. Experimental

2.1. Material used

Aluminum alloy 1050, with the nominal chemical composition of (in wt%) 0.29% Fe, 0.15% Si, 0.02% Ti, 0.02% Zn, 0.01% Mg, 0.01% Ni was used in this work. Specimens with dimensions of 1 mm × 20 mm × 30 mm were cut from an extruded bar, with the surface facing towards the normal direction of the slab. The samples were electropolished in a solution composed of 80 vol% ethanol and 20 vol% perchloric acid solution at 10 °C and 20 V for 240 s, in order to produce a smooth surface for the development of well-ordered pore structures during anodization.

2.2. Coating procedure

The deposition of electroless Ni-P coating was studied with three different processes, as summarized in Fig. 1. Ni-P was coated on (i) electropolished surfaces, (ii) electropolished and then anodized surfaces, and (iii) electropolished, anodized and activated surfaces. Activation was done by immersion in nickel fluoride solution, and the coating of Ni-P was done using the solution as given in Table 1, for 1 h at 85 ± 2 °C. The solution was continuously stirred to remove the hydrogen gas generated during the coating process. Each coating process was monitored and controlled during experiment to have identical experimental conditions. For the single pre-treatment procedure, anodizing was performed in 2 M sulfuric acid solution using a constant voltage of 15 V at 20 ± 2 °C for 300 s, followed by Ni-P coating. For Ni-P coating with double pre-treatment, anodized samples were surface-activated by immersion in 5 g/l nickel fluoride tetrahydrate ($NiF_2{\cdot}4H_2O$) solution at 30 ± 1 °C and pH 6 ± 0.2 for 60, 120, and 240 s. The effect of surface activation was further investigated to better understand and optimize the Ni-P coating.

2.3. Characterization of the coating

Microstructure evolution, chemical composition, thickness, and roughness of the coated specimens were investigated using a ZEISS Ultra 55 SEM, equipped with an energy-dispersive X-ray spectroscopy (EDS) detector from Oxford Instruments, operated with INCA program, and the Keyence VK-X200K CLM. The analyses were performed on both top view surfaces and cross sections of coated specimens. Cross sections were obtained by sectioning the specimens using ultramicrotomy in order to observe the intermediate oxide layer without preparation artefacts. The SEM was used to image the coating in cross-sectional view and to measure precisely its thickness and morphology. The ImageJ and

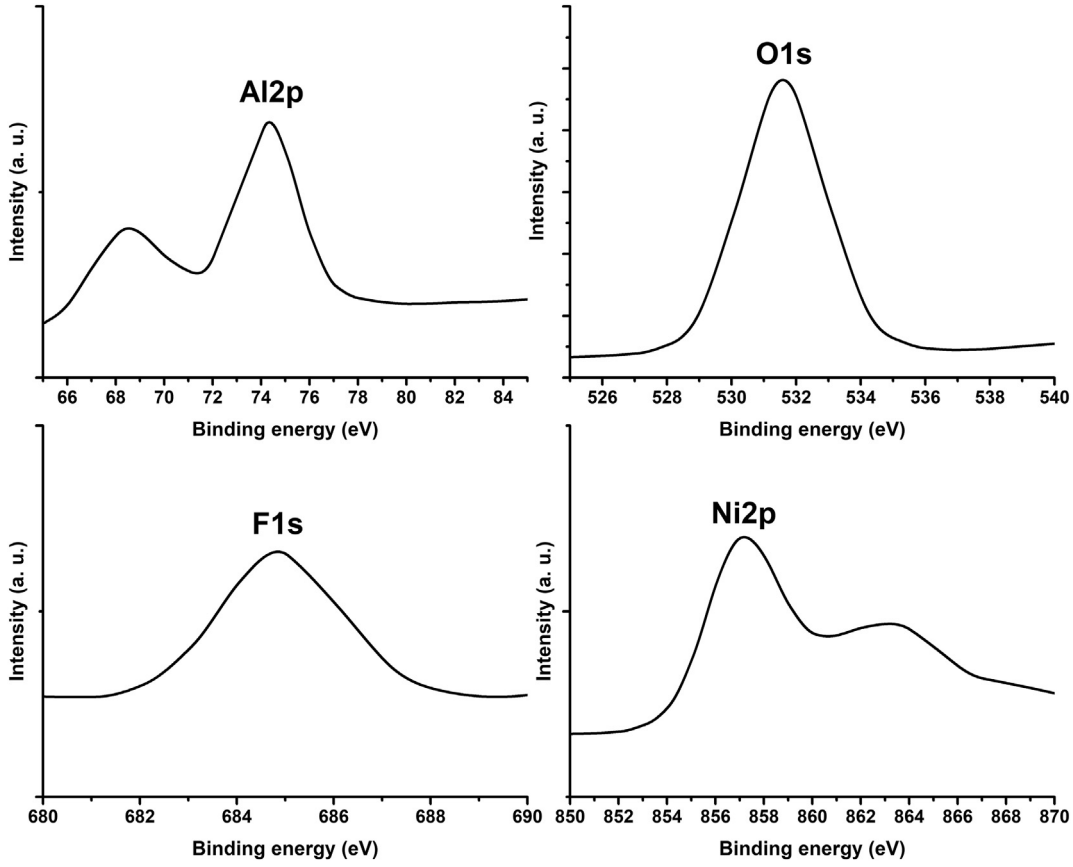

Fig. 4. XPS spectra for Al2p, O1s, F1 s, and Ni2p signals of the anodized + activated/sealed sample.

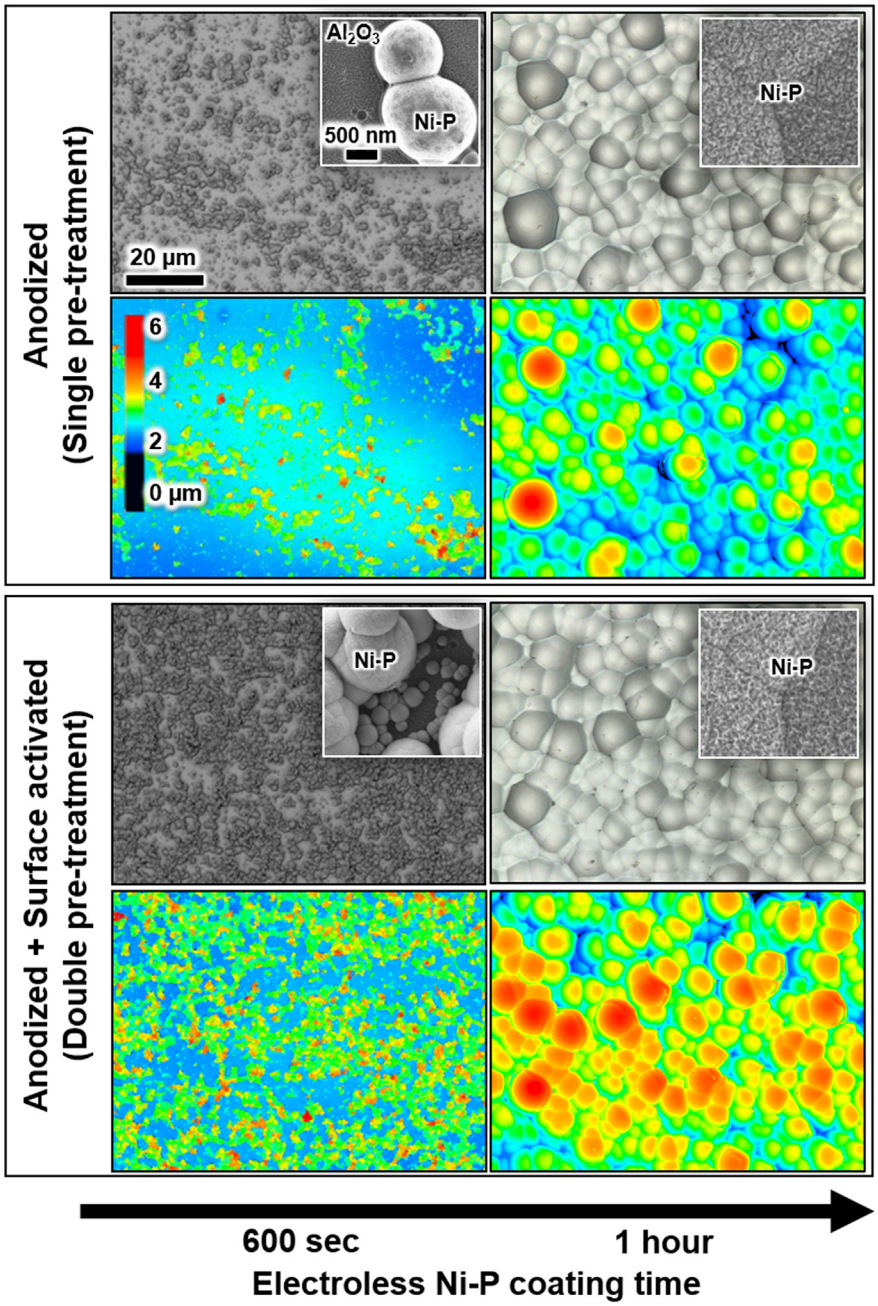

Fig. 5. Surface morphology of the Ni-P coating showing the effect of activation and coating time of nickel. The scale bars in top left figures applies to all other figures. All images were taken at the same magnification.

Table 2
Thickness and roughness of the Ni-P coating as a function of pre-treatment.

Pre-treatment type	Thickness (µm)	Roughness before coating (nm)	Roughness after coating (nm)
No pre-treatment[a]	22.3 ± 0.9	60 ± 5	276 ± 43
Non-activated (single pre-treatment)	15.3 ± 0.7	86 ± 8	259 ± 11
Activated (double pre-treatment)	17.8 ± 0.7	86 ± 7	258 ± 10

[a] Significant spallation occurred in large areas.

VK Analyzer software were used to calculate the coating thicknesses. XRD measurements were carried out to obtain structural information before and after electroless Ni-P coating. The film composition was further investigated by X-ray photoelectron spectroscopy (XPS) using a Thermo Scientific X-ray Photoelectron Spectrometer. Vickers microhardness tests were performed to measure the hardness of the coating using a load of 50 g ($HV_{0.05}$) on the surface of the coating as well on its cross section, with the arithmetic mean reported as the average hardness. Scratch tests were carried out to determine the adhesion behavior of the coatings using the Teer Coatings ST-3001 testing system with loads between 1 and 30 N. Post CLM surface examinations of scratching was done to determine the critical load (*Lc*), defined as the force

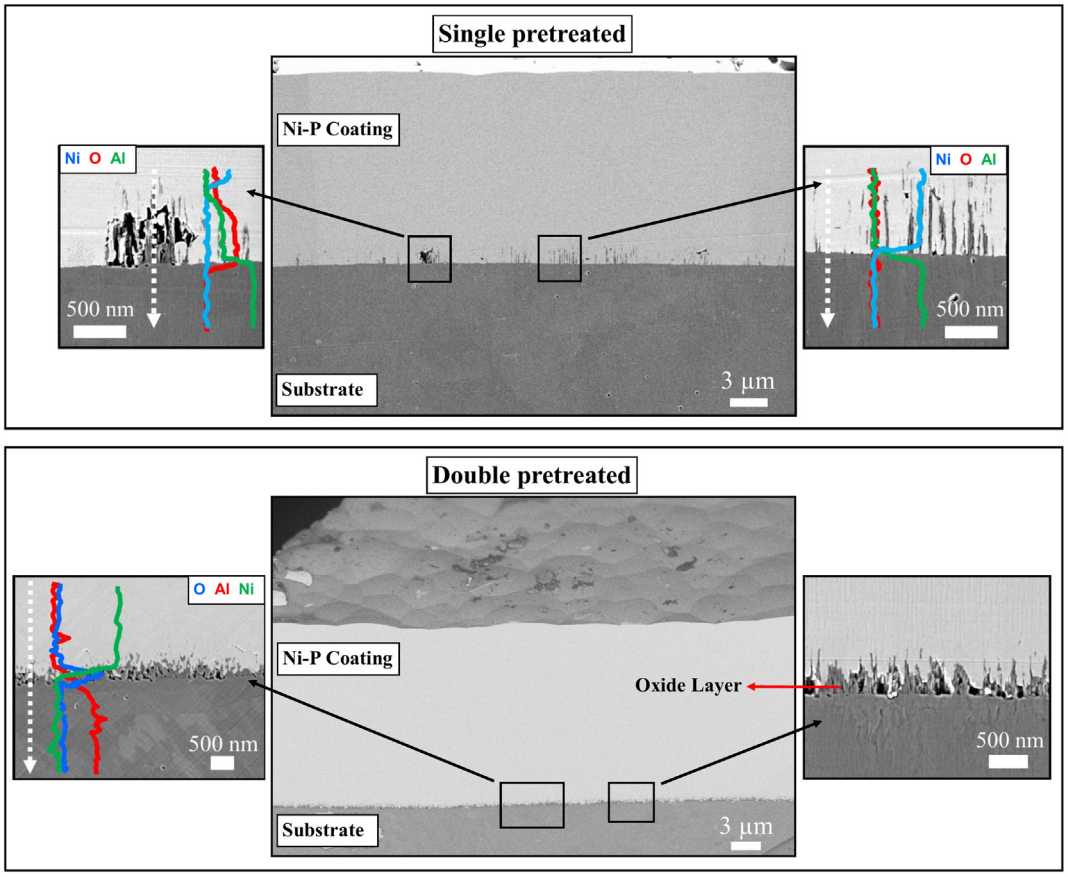

Fig. 6. Cross-sectional SEM images with EDS line scan analyses of the Ni-P coating deposited via single and double pre-treatment.

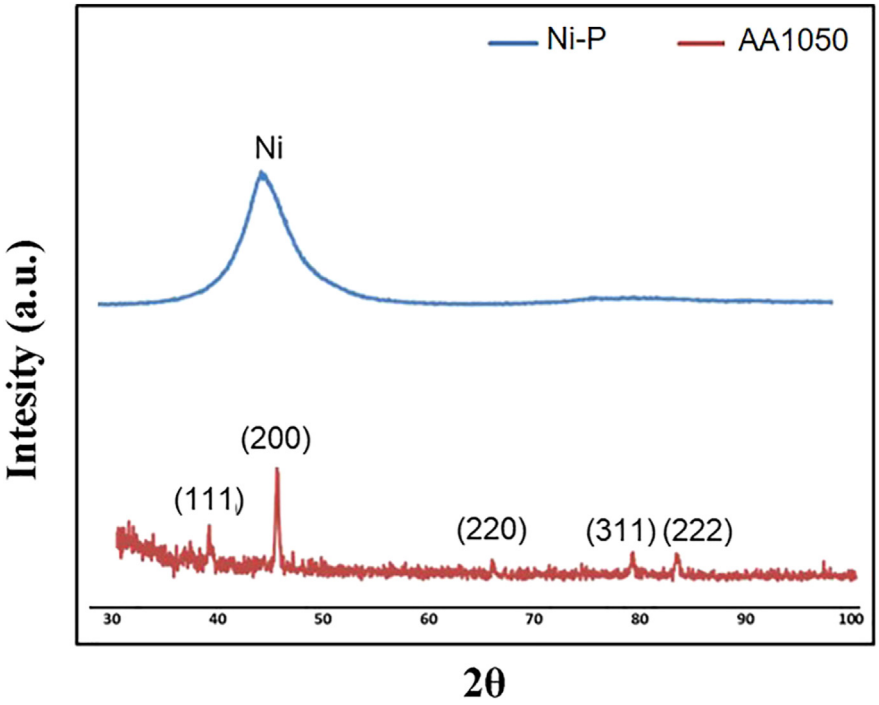

Fig. 7. XRD spectra from the AA1050 aluminum alloy and electroless Ni-P coating after double pre-treatment.

causing cracking and expanding across the entire deformed scratch area. Friction tests by reciprocating against a steel ball (5 mm diameter) were carried out using a tribometer from Bruker UMT with 1 N load. The coefficient of friction (COF) at room temperature was determined out from 300 cycles with a total travel distance of 3 m carried out within 20 min. Wear tests were carried out using the pin-on-disc method in ambient air using a WC-6Co abrasive tip. The pin tip was placed orthogonally on the specimen with a constant load of 5 N and

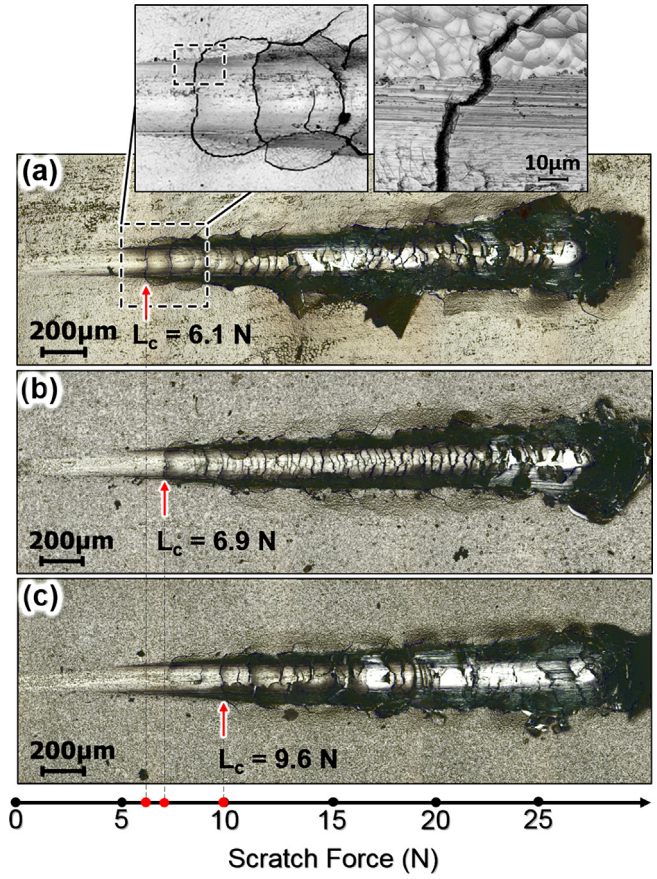

Fig. 8. CLM images taken after scratch test of the coated specimens with (a) no pre-treatment, (b) single pre-treatment (only anodized), (c) double pre-treatment (anodized + surface-activated).

rotated with a speed of 100 rpm. The experiment was terminated when delamination of the coating occurred. The volumes of the wear tracks were measured using the VK Analyzer software and the wear factor (k) determined using the following formula [27,28]:

$$k = \frac{V}{F \times L} \tag{1}$$

with k being the wear factor (mm^3/N·m), V the wear track volume (mm^3), F the applied load (5 N), and L the wear distance (m).

3. Results and discussion

3.1. Surface morphology after electropolishing and pre-treatments

Rolling lines and scratches were almost entirely removed by electropolishing, producing a smooth and clean surface (Fig. 2a–b). The average surface roughness (Ra) decreased from 411 ± 14 nm to 60 ± 5 nm. Anodizing resulted in an oxide film with 1.5 μm thickness being highly uniform and having nanometer-sized pores (Fig. 2c). The sealing treatment by immersion in nickel fluoride was able to close ≈20% of all pores, as shown in Fig. 2d. > 80% of surface pore closure was achieved after 120 s (Fig. 2e), and ≈99% of the pores were closed after 240 s, as illustrated in Fig. 2f. A previous study indicated that 120 s of surface activation treatment leads to optimum pore closure which it is suitable for electroless Ni-P coating [3]. Cross-sectional imaging of the coating demonstrated that the sealing treatment was successful in pore closure without affecting the oxide thickness (Fig. 3). Hence, the treatment with nickel fluoride reduced the micro-porosity in the aluminum oxide and resultant in improved quality of the nickel coating.

3.2. Composition of the coating

XPS spectra for Al2p, O1s, F1s and Ni2p are presented in Fig. 4, confirming the presence of these elements in the surface. The Al2p peak at 74.28 eV and O1s peak at 531.48 eV refer to Al_2O_3 (oxide film) and aluminum hydroxide, respectively, and indicate their presence in the surface [29]. The Ni2p peak at 857.24 eV is the typical binding energy for nickel hydroxide [26,30]. The F1s peak signal at 684.95 eV suggests its presence in the form of nickel fluoride [31]. However, it is also likely that aluminum fluoride was present as suggested by the broad F1s peak is at 687.75 eV [32–35]. The presence of aluminum hydroxide [$Al(OH)_3$], nickel hydroxide [$Ni(OH)_2$], and aluminum fluoride (AlF_3) cannot be excluded as these are typical by-products of the deposition process which can be incorporated into the coating and seal the pores [23,25,36].

3.3. Surface morphology after electroless Ni-P coating

Fig. 5 shows the surface morphology of the nickel coating as a function of coating time with and without surface activation. Surface activation increased the coating efficiency, favoring the deposition of Ni-P. The coating after 600 second immersion time was incomplete for both conditions, but the activator increased the surface coverage. After 1 h of deposition, the Ni-P coating covered entirely the surface for both conditions. The thickness of the coating, surface-activated, was 17.8 ± 0.7 μm whereas the thickness was 15.3 ± 0.7 μm when the surface was non-activated. Roughness and thickness measurement

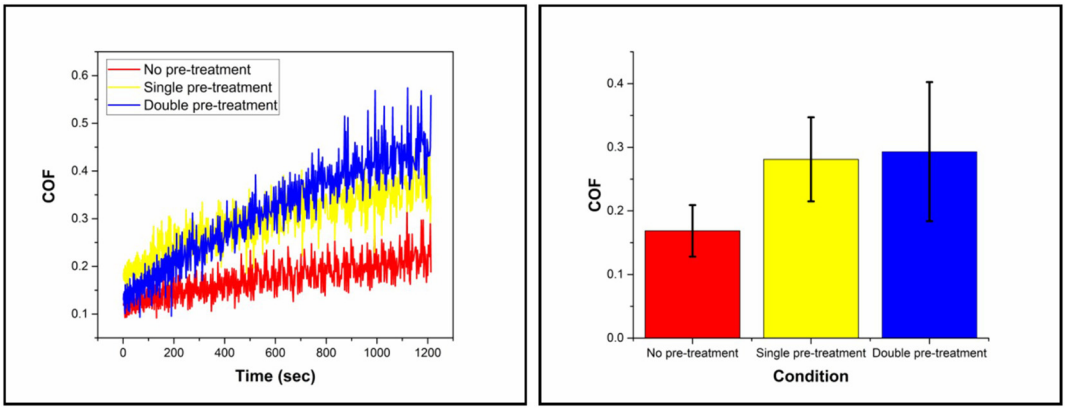

Fig. 9. The behavior of the coefficient of friction (COF) of the nickel coating, deposited via different pre-treatment, as a function of time.

Table 3
Wear test results for electroless Ni-P coatings using three different conditions.

Pre-treatment type	Wear track volume, V (mm^3)	Wear distance, L (m)	Wear factor, k (mm^3/Nm)
No pre-treatment	0.262	80	6.55×10^{-4}
Non-activated (single pre-treatment)	0.474	164	5.78×10^{-4}
Activated (double pre-treatment)	0.104	572	3.64×10^{-5}

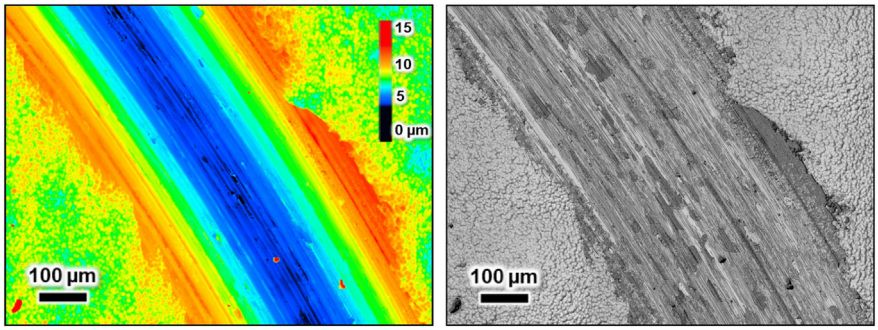

Fig. 10. CLM surface images of electroless Ni-P coating deposit after double pre-treatment showing abraded material after testing for the wear resistance tested using the pin-on-disc method.

results were summarized in Table 2. Surface activation, apparently, had no influence on surface roughness. Nodular, cauliflower-like structures, being typical for electroless Ni-P coating, were observed on the surface after both pre-treatment conditions (Fig. 5).

3.4. Morphology and structure of the Ni-P coating

The thickness of the electroless Ni-P coating in sample coated without pre-treatment was greater compared to the single and double pretreated samples, as seen in Table 2. When Ni-P was deposited directly on the surface of aluminum without pre-treatment, it accumulated relatively loosely on the surface, resulting in a more porous structure with greater thickness. Similar results were reported by Wang and Wu [13]. Double pre-treatment, however, resulted in thicker nickel deposition. This can be explained by partial dissolution of the oxide which occurs during single pre-treatment, leading to loss of continuity, causing delay of the nucleation and deposition process. The adhesion of the nickel coating without any pre-treatment was weak so that exfoliation occurred which makes this deposition method out of question due to quality concerns. Cross-section images of the Ni-P coating as a function of pre-treatment are shown in Fig. 6. EDS line scan analyses revealed the presence of oxygen beneath the Ni-P coating for both single and double pre-treated conditions. This indicates that an intermediate residual oxide layer, formed due to the anodic oxidation, remained after nickel deposition. The oxide layer beneath the coating deposited after single pre-treatment had more flaws than after double pre-treatment, clearly showing the beneficial activation effect of nickel fluoride. EDS analyses confirmed the presence of phosphorus (> 12 wt %) in all coatings. XRD diffraction patterns of uncoated AA1050 and the Ni-P coating are summarized in Fig. 7. Good peak match of indexed diffraction signals, corresponding to aluminum, was obtained. The Ni-P-coated substrate, in contrast, showed only a broad peak with a width of ca. 20° 2-theta, indicating amorphous nickel [37,38]. No signal from the bulk aluminum [7,39] was seen indicating a successful coating of a thickness of at least 15 µm.

3.5. Mechanical properties of the coating

The hardness of the substrate was $47 \pm 5\ HV_{0.05}$. The hardness of the nickel coating was for all pre-treated conditions $522 \pm 19\ HV_{0.05}$. The adhesion behavior, as summarized in Fig. 8, of the nickel coating, doubly pretreated, was more superior to the coating singly pretreated, as apparent from the *Lc* value showing 9.6 N for double pre-treatment (surface activated) and 6.9 N for single pre-treatment. The *Lc* on the substrate without any pre-treatment was 6.1 N. This, hence, showed that the surface activation treatment improved the adhesion of the Ni-P coating to the substrate. Electroless Ni-P coated on anodized aluminum was also demonstrated to show improved adhesion properties and explained as a mechanical interlocking effect between anodized layer and nickel coating [19]. The pores in the aluminum oxide are, hence, beneficial for a stronger adhesion.

Fig. 9 summarizes the friction measurement results. The COF increased with increasing reciprocating time for all deposited nickel coating, with the pretreated substrates, however, showing higher friction performance than the non-pretreated condition. The COF of singly and doubly pretreated conditions increased similarly with the latter seemingly reaching higher COF values. This is in well-agreement with the work of Liu et al. [40] who also observed high COF on electroless Ni-P coating doubly pretreated and attributed this to the roughness contributing to higher friction. The roughness of the coating for both pretreated conditions was practically the same which may explain the similar COF values of both conditions (Table 3).

The wear test results are summarized in Table 3 and Fig. 10. The coating with no pre-treatment showed the lowest wear resistance ($3.64 \times 10^{-5}\ mm^3$/Nm), and the coating with double pre-treatment exhibited the highest wear resistance ($6.55 \times 10^{-4}\ mm^3$/Nm). The nickel fluoride treatment resulted in a more well-structured intermediate oxide layer at the substrate-coating interface (Fig. 6), demonstrating that the Ni-P coating adhered well to the substrate, which potentially explains the reason for the improved wear behavior.

4. Conclusions

The use of nickel fluoride as an activator and sealant for the coating of electroless Ni-P on anodized AA1050 aluminum alloy showed following beneficial properties:

- Ni-P was more efficiently deposited on anodized substrates due to improved morphology and structure at the oxide/coating interface.
- The Ni-P coating showed larger coefficient of friction indicating improved resistance against friction.
- The Ni-P coating showed improved wear resistance and adhesion properties.

Acknowledgement

The authors are grateful for financial support from TÜBİTAK (The Scientific and Technological Research Council of Turkey) through the scholarship grant number 1059B14140108 and the project no. 114M063. The authors are also grateful for EPSRC for financial support through LightForm program grant no. EP/R001715/1. M.K. and N.C. express their gratitude Yildiz Technical University for financial support through project no. 2014-07-02-DOP02. M.K. would like address special thanks to Dr. Şavklıyıldız, Konya Technical University, for valuable discussion.

References

[1] R. Kang, Z. Peng, B. Liu, D. Wang, J. Liang, A protocol for fast electroless Ni-P on Al alloy at medium-low temperature accelerated by hierarchically structured Cu immersion layer, Surf. Coatings Technol. 309 (2017) 67–74, https://doi.org/10.1016/j.surfcoat.2016.11.029.

[2] G. Sheng, Study on growth mode and properties of electroless nickel plating on aluminum alloy, Chem. Eng. Trans. 55 (2016) 319–324, https://doi.org/10.3303/CET1655054.

[3] M. Kocabaş, PhD Thesis, Properties of Pre-treated Electroless Nickel and Bor Nitride Reinforced Electroless Nickel Coatings on Anodized Aluminum Surface, Yildiz Technical University, 2017.

[4] J. Sudagar, J. Lian, W. Sha, Electroless nickel, alloy, composite and nano coatings - a critical review, J. Alloys Compd. 571 (2013) 183–204, https://doi.org/10.1016/j.jallcom.2013.03.107.

[5] S.B. Sharma, R.C. Agarwala, V. Agarwala, K.G. Satyanarayana, Characterization of carbon fabric coated with Ni-P and Ni-P-ZrO2-Al2O3 by electroless technique, J. Mater. Sci. 37 (2002) 5247–5254, https://doi.org/10.1023/A:1021056503872.

[6] B. Zhang, Amorphous and Nano Alloys Electroless Depositions, Elsevier, Changsha, 2016. https://www.elsevier.com/books/amorphous-and-nano-alloys-electroless-depositions/zhang/978-0-12-802685-4.

[7] Z. Yin, F. Chen, Effect of nickel immersion pretreatment on the corrosion performance of electroless deposited Ni-P alloys on aluminum, Surf. Coatings Technol. 228 (2013) 34–40, https://doi.org/10.1016/j.surfcoat.2013.04.001.

[8] D. Takacs, L. Sziraki, T.I. Török, J. Solyom, Z. Gacsi, K. Gal-Solymos, D. Takács, L. Sziráki, T.I. Török, J. Sólyom, Z. Gácsi, K. Gál-solymos, Effects of pre-treatments on the corrosion properties of electroless Ni-P layers deposited on AlMg2 alloy, Surf. Coatings Technol. 201 (2007) 4526–4535, https://doi.org/10.1016/j.surfcoat.2006.09.045.

[9] S.-Y.Y. Tsai, C.-H.H. Lin, Y.-J.J. Jian, K.-H.H. Hou, M.-D. Der Ger, The fabrication and characteristics of electroless nickel and immersion Au-polytetrafluoroethylene composite coating on aluminum alloy 5052 as bipolar plate, Surf. Coatings Technol. 313 (2017) 151–157, https://doi.org/10.1016/j.surfcoat.2017.01.064.

[10] M. Hino, K. Murakami, Y. Mitooka, K. Muraoka, T. Kanadani, Effects of zincate treatment on adhesion of electroless Ni-P coating onto various aluminum alloys, Mater. Trans. 50 (2009) 2235–2241, https://doi.org/10.2320/matertrans.L-M2009819.

[11] A. Farzaneh, M. Sarvari, M. Ehteshamzadeh, O. Mermer, Effect of zincating bath additives on structural and electrochemical properties of electroless Ni-P coating on AA6061, Int. J. Electrochem. Sci. 11 (2016) 9676–9686, https://doi.org/10.20964/2016.11.75.

[12] S. Court, C. Kerr, C. Ponce de León, J.R. Smith, B.D. Barker, F.C. Walsh, Monitoring of zincate pre-treatment of aluminium prior to electroless nickel plating, Trans. Inst. Met. Finish. 95 (2017) 97–105, https://doi.org/10.1080/00202967.2016.1236573.

[13] J. Wang, Q. Wu, The effects of anodic interlayer on the morphology and mechanical performances of electroless Ni–P coating on Al alloy, Appl. Phys. A Mater. Sci. Process. 123 (2017) 435, , https://doi.org/10.1007/s00339-017-1048-5.

[14] G. Szirmai, J. Tóth, T.I. Török, N. Hegman, An experimental study on the effect of aqueous hypophosphite pre-treatment used on an aluminium alloy substrate before electroless nickel plating, Mater. Sci. Forum 659 (2010) 103–108, https://doi.org/10.4028/www.scientific.net/MSF.659.103.

[15] C. Subramanian, K. Palaniradja, Effect of surfactant on the electroless Ni-P/Ni-B duplex coatings on aluminium 7075, Int. J. Metall. Eng. 2015 (2015) 25–32, https://doi.org/10.5923/j.ijmee.20150402.01.

[16] J.G. Jin, S.K. Lee, Y.H. Kim, Adhesion improvement of electroless plated Ni layer by ultrasonic agitation during zincating process, Thin Solid Films 466 (2004) 272–278, https://doi.org/10.1016/j.tsf.2004.02.100.

[17] V. Vitry, A. Sens, A.-F.F. Kanta, F. Delaunois, Wear and corrosion resistance of heat treated and as-plated Duplex NiP/NiB coatings on 2024 aluminum alloys, Surf. Coatings Technol. 206 (2012) 3421–3427, https://doi.org/10.1016/j.surfcoat.2012.01.049.

[18] J. Sudagar, K. Venkateswarlu, J. Lian, Dry sliding wear properties of a 7075-T6 aluminum alloy coated with Ni-P (h) in different pretreatment conditions, J. Mater. Eng. Perform. 19 (2010) 810–818, https://doi.org/10.1007/s11665-009-9545-0.

[19] S. Shirmohammadi Yazdi, F. Ashrafizadeh, A. Hakimizad, Improving the grain structure and adhesion of Ni-P coating to 3004 aluminum substrate by nanostructured anodic film interlayer, Surf. Coatings Technol. 232 (2013) 561–566, https://doi.org/10.1016/j.surfcoat.2013.06.028.

[20] H. Jha, T. Kikuchi, M. Sakairi, H. Takahashi, Palladium nanoparticle seeded electroless metallization of Al/Al2O3 surfaces, Mater. Lett. 63 (2009) 1451–1454, https://doi.org/10.1016/j.matlet.2009.03.046.

[21] I.V. Gordovskaya, T. Hashimoto, J. Walton, M. Curioni, G.E. Thompson, P. Skeldon, Development of cerium-rich layers on anodic films formed on pure aluminium and AA7075 T6 alloy, J. Electrochem. Soc. 161 (2014) C601–C606, https://doi.org/10.1149/2.0091501jes.

[22] A. Carangelo, M. Curioni, A. Acquesta, T. Monetta, F. Bellucci, Cerium-based sealing of anodic films on AA2024T3: effect of pore morphology on anticorrosion performance, J. Electrochem. Soc. 163 (2016) C907–C916, https://doi.org/10.1149/2.1001614jes.

[23] Y. Zuo, P. Zhao, J. Zhao, The influences of sealing methods on corrosion behavior of anodized aluminum alloys in NaCl solutions, Surf. Coatings Technol. 166 (2003) 237–242, https://doi.org/10.1016/S0257-8972(02)00779-X.

[24] J. Lee, Y. Kim, J. Kim, W. Chung, Effect of sealing on thermal conductivity of aluminium anodic effect of sealing on thermal conductivity of aluminium anodic oxide layer, J. Nanoelectron. Optoelectron. 9 (2014) 9136–9140, https://doi.org/10.1166/jno.2014.1563.

[25] L. Hao, B.R. Cheng, Sealing processes of anodic coatings-past, present, and future, Met. Finish. 98 (2000) 8–18 http://linkinghub.elsevier.com/retrieve/pii/S0026057601800027.

[26] J. Gonzalez, S. Feliu Jr, A. Bautista, E. Otero, and S. Feliu. Changes in cold sealed aluminium oxide films during ageing. J. Appl. Electrochem. 29 (1999) 845–854. doi:https://doi.org/10.1023/A:1003569330080.

[27] M.S.T. Pires, T. Doca, V.F. Steier, W.M. da Silva, M.M.O. Júnior, Wear resistance of coated SAE 305 aluminum alloy under dry friction reciprocate sliding, Tribol. Lett. 66 (2018) 1–11, https://doi.org/10.1007/s11249-018-1000-7.

[28] O.A. León, M.H. Staia, H.E. Hintermann, Wear mechanism of Ni-P-BN(h) composite autocatalytic coatings, Surf. Coatings Technol. 200 (2005) 1825–1829, https://doi.org/10.1016/j.surfcoat.2005.08.061.

[29] J. Zähr, S. Oswald, M. Türpe, H.J. Ullrich, U. Füssel, Characterisation of oxide and hydroxide layers on technical aluminum materials using XPS, Vacuum. 86 (2012) 1216–1219, https://doi.org/10.1016/j.vacuum.2011.04.004.

[30] A.P. Grosvenor, M.C. Biesinger, R.S.C. Smart, N.S. McIntyre, New interpretations of XPS spectra of nickel metal and oxides, Surf. Sci. 600 (2006) 1771–1779, https://doi.org/10.1016/j.susc.2006.01.041.

[31] M.C. Biesinger, L.W.M. Lau, A.R. Gerson, R.S.C. Smart, The role of the Auger parameter in XPS studies of nickel metal, halides and oxides, Phys. Chem. Chem. Phys. 14 (2012) 2434–2442, https://doi.org/10.1039/c2cp22419d.

[32] A. Limcharoen, C. Pakpum, P. Limsuwan, An X-ray photoelectron spectroscopy investigation of redeposition from fluorine-based plasma etch on magnetic recording slider head substrate, Procedia Eng. 32 (2012) 1043–1049, https://doi.org/10.1016/j.proeng.2012.02.052.

[33] O. Böse, E. Kemnitz, A. Lippitz, W.E.S. Unger, C 1s and Au 4f 7/2 referenced XPS binding energy data obtained with different aluminium oxides, -hydroxides and -fluorides, Fresenius J. Anal. Chem. 358 (1997) 175–179, https://doi.org/10.1007/s002160050376.

[34] A. Makarowicz, C.L. Bailey, N. Weiher, E. Kemnitz, S.L.M. Schroeder, S. Mukhopadhyay, et al., Electronic structure of Lewis acid sites on high surface area aluminium fluorides: a combined XPS and *ab initio* investigation, Phys. Chem. Chem. Phys. 11 (2009) 5664–5673, https://doi.org/10.1039/b821484k.

[35] J. Sun, J. Shao, K. Yi, W. Zhang, Effects of substrate temperatures on the characterization of magnesium fluoride thin films in deep-ultraviolet region, Appl. Opt. 53 (2014) 1298–1305, https://doi.org/10.1364/AO.53.001298.

[36] M.R. Kalantary, D.R. Gabe, D.H. Ross, A model for the mechanism of nickel fluoride cold sealing of anodized aluminium, Plat. Surf. Finish. 80 (1993) 52–56, https://doi.org/10.1007/BF01030188.

[37] Z. Rajabalizadeh, D. Seifzadeh, Application of electroless Ni-P coating on magnesium alloy via CrO3/HF free titanate pretreatment, Appl. Surf. Sci. 422 (2017) 696–709, https://doi.org/10.1016/j.apsusc.2017.06.100.

[38] C. Yanhai, C. Hengyang, Tribological behavior of Ni-P deposits on dry condition, Rare Met. Mater. Eng. 43 (2014) 11–16, https://doi.org/10.1016/S1875-5372(14)60043-6.

[39] C.-I.I. Hsu, K.-H. Hou, M.-D. Ger, G.L. Wang, The effect of incorporated self-lubricated BN(h) particles on the tribological properties of Ni-P/BN(h) composite coatings, Appl. Surf. Sci. 357 (2015) 1727–1735, https://doi.org/10.1016/j.apsusc.2015.09.207.

[40] Z. Liu, W. Gao, Electroless nickel plating on AZ91 Mg alloy substrate, Surf. Coatings Technol. 200 (2006) 5087–5093, https://doi.org/10.1016/j.surfcoat.2005.05.023.